Aerodynamic Lift Railcar Suspension – Faster, Quieter, More-Efficient

Abstract

Ground effect flight becomes increasingly efficient as the vehicle-ground gap decreases and the lateral losses of the vehicle's lower surface lift pressures are blocked. For light railcars with 95%-99% of the weight suspended by aerodynamic forces, rubber tires may be used without excessive wear for quieter and faster transit. Computational Fluid Dynamics (CFD) simulation of 3D digital prototypes have shown that lift-to-drag efficiencies 3X that of the best airliners are possible which translates to energy consumption about half of the best high-speed rail.

The research of this paper identifies the best performance is attained with design features of: a) a lower surface compartment defined on the sides by a track-fence wall and on the aft with a trailing edge flap, b) an upper surface distributed fan propulsion in combination with wheel propulsion, and c) a frontal vehicle section that both directs air into the lower surface compartment creates induced thrust from expansion of air upward from the vehicle's frontal stagnation point. While high-speed rail is very energy efficient, the use of distributed propulsion to create induced thrust is able to reduce energy consumption by 50%, even at higher speeds. Efficiency is even higher for transit in tunnels.

Introduction

Traditional theories on how air flow creates aerodynamic lift have implied that wings and turning air flow are critical. The results of this research rebuff former theories in lieu of an axiom that identifies the impacting and diverging of air flow with surfaces to create higher and lower pressures is the underlying basic physics that creates lift forces. This axiom has been mutually validated by continuum and discrete mechanics and accurately extrapolates—this level of validation makes it more than a theory. This axiom teaches toward ground effect flight of railcars as being the most efficient mode of high-speed transit.

Ground effect flight is more efficient than free flight because the ground blocks the downward direction loss of lift pressures; however, the most common wing-in-ground (WIG) craft are maritime aircraft where waves limit the approach to water's surface and lateral loss of lift pressures can be significant. Transit over rails overcome these WIG-over-water limitations where the rails both allow transit close to the ground and block lateral losses of lift pressures. Existing rail structure may be used for these new generation WIG railcars, including access via subways throughout cities.

Figure 1 illustrates a WIG railcar with lower surface fences aligned in close proximity to rails to reduce lateral losses of lift pressure. Figure 2 illustrates the pressure profile of a 2D CFD simulation with higher pressures on lower surfaces and lower pressure on upper surfaces.

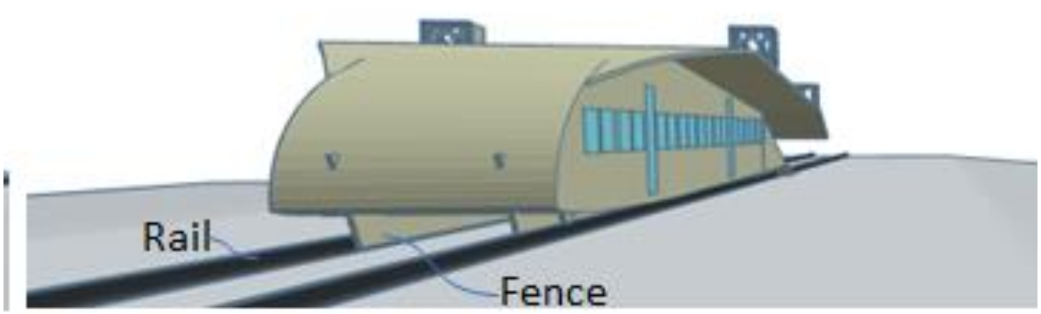

Figure 1. Image of flying rail car.

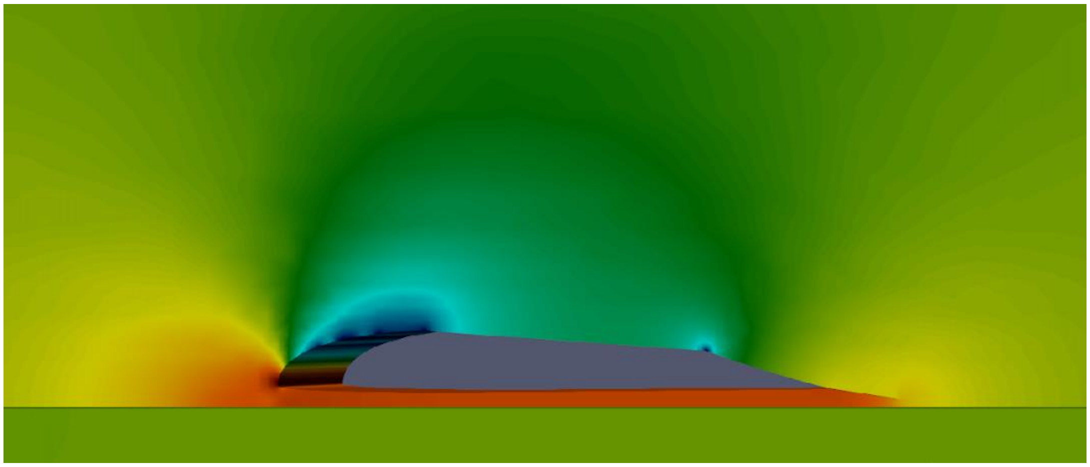

Figure 2. Proof of concept pressure profile of railcar airfoil flying above the flat surface between rails. Pressures from low to high progress from blue to red.

Background

CFD are an accepted and good standard method for characterizing the performance of aircraft by simulating the performance of digital prototypes.[1, 2] The fundamental problem with 2D CFD is that wing performance is typically dominated by losses of lift over side edges which are not accounted-for in 2D simulations.[3-6] This research uses 2D CFD simulations to gain insight into performance trends followed by more-rigorous 3D simulations of digital prototypes representative of actual WIG railcars.

2D CFD Toward Understanding Aerodynamic Lift – Air flow is converted to aerodynamic lift per the following four heuristics [7]:

Heuristic 1. Air velocities impacting surfaces increase surface pressures.

Heuristic 2. Air velocities diverging from surfaces decrease surface pressures (by creating voids).

Heuristic 3. Air flows from higher to lower pressures (at the speed of sound); this pressure-driven flow joins with other air flows to form complex streamlines.

Heuristic 4. The L/D of a section of an airplane surface is approximately equal to 57° divided by the pitch of the surface in degrees for lower surfaces and -57° divided by the pitch for upper surfaces. The pitch angle is relative to horizontal with the nose up as positive.

Heuristic 4 allows qualitative observations on pressure profiles from 1-3 to be quantified to L/D efficiency.

The Figure 2 pressure profile is most complex, but all phenomena can be explained by Heuristics 1-3. The higher pressures on the lower surface are the result of the ground blocking the loss of lift pressures in the downward direction, and the expression of the higher pressures on a mostly horizontal lower surface results in high L/D efficiency.

Lower pressures form on the upper surfaces of the frontal section due to expanding air diverging from those surfaces. These lower pressures induce thrust which further increases L/D efficiency.

Boundary Layer – As a correcting detail, the only air streamlines that collide or diverge from surfaces are those streamlines in a thin boundary layer. Beyond that boundary layer, molecule-molecule collisions in the gas phase transfer pressures and form pressure gradients.

The impacting and diverging of airflow vectors with a surface are continuum mechanics descriptions of the processes that generate aerodynamic lift. The collision of air molecules with the resulting formation of pressure gradients is a kinetic theory of gases explanation. The above 1-6 stages are consistent from both the continuum mechanics perspective and from the kinetic theory of gas perspective.

Kinetic Theory of Gases – The continuum-level Heuristics 1-3 are validated on the discrete level of gas molecules through the following restatements in terms of the kinetic theory of gases:

Heuristic 1. Air molecules having random translational directions have increased velocities relative to an approaching airfoil; therefore, the momentum of the molecules relative to the leading edge are increased by a value proportional to the approach speed with a corresponding increase in force caused by the impact of those molecules on leading surfaces. Stated in terms of continuum mechanics, *impacting flow causes higher pressures*.

Heuristic 2. In the absence of translational movement of air molecules, an airfoil would create a perfect vacuum in its wake—similar to the way a snow plow leaves a cleared snow path in its wake. In practice, gas molecules flow into the wake and convert that "perfect vacuum" into a lower pressure region. Stated in terms of continuum mechanics, *diverging flow causes lower pressures*.

Heuristic 3. At room temperature, gas molecules translate 500 m/sec in random directions; the speed of sound in a gas is 340 m/sec which is basically a conversion from random to directional transit. Thus, gases have a net flow through pressure gradients at about the speed of sound. Stated in terms of continuum mechanics, *air flows from higher to lower pressures at the speed of sound*.

These qualitative verifications can become quantitative through Monte Carlo simulation which is computationally intensive and outside the scope of this paper.[8-11]

Key Performance Features - The fence-rail transition is a key design degree of freedom. Key parameters for study in instant paper include:

- Airfoil shapes which are illustrated in the pressure profile results and which are constant across the span of the cabin.
- Free stream air flow, 40 m/s unless otherwise identified, at a boundary condition sufficiently distant (i.e., free stream air velocity) so as not to be influenced by the digital prototype. The free stream pressure is 1 atm. Unless otherwise stated the length of the cabin (including rear flap) is 6.4m.
- The "clearance ratio" (CR), which is the distance between the lowest surface of the cabin or flap and the ground divided by the maximum height (i.e. thickness) of the cabin (excluding flap). The "Gap Ratio" is the distance from the cabin without flap to the ground divided by thickness.
- The "Flap %" which is the percent of the total gap blocked by a trailing edge flap.

Experimental Methods

The experimental investigation consisted of computational fluid dynamic (CFD) studies of 2D and 3D digital prototypes of a lifting-body vehicle cabin suitable for passenger or cargo payloads.

An efficient lift-generated compartment is formed in flight. It is defined on the sides by the rail-fence wall, on the trailing section by the flap, and on the lead section by an open gap in which oncoming air flows into the compartment. The vehicle's lower surface and ground (or any surface between the rails) form the upper and lower compartment surfaces. Air flows out of the compartment under the trailing edge flap in 2D CFD simulation. In 3D CFD simulation air flows out in the gap between the fences and rails in addition to under the trailing-edge flap.

Results from CFD simulations (i.e., experiments) include: lift coefficients (C_l), drag coefficients (C_d), L/D (equal to C_l/C_d), pressure profile images, and velocity profile images. Flow around wheels on the vehicle is not considered under the assumption that air flow can be streamlined between fences and wheels.

Digital prototype simulations are designed per the following sequence:

1. 2D CFD airfoil studies to understand trends in C_l, C_d, and L/D for a thick airfoil in the proximity of ground.
2. 3D CFD lifting body studies (i.e., cabin with constant airfoil cross section) to understand how to preserve high airfoil L/D to WIG railcar applications.
3. Studies to understand limits of performance that can be used to identify viable designs and operating conditions.

Results and Preliminary Discussions

2D CFD Studies - Figure 3 and Table 1 summarize how the distance between the airfoil and the ground impacts performance. The distance is characterized by the clearance ratio (CR). Lower clearance ratios lead to higher pressures and therefore higher L/D. The blocking of lift pressures in the downward direction has a significant and beneficial impact on L/D and C_l. An ideal seal against lateral loss of lift pressures is implicit in these 2D simulations.

The trailing edge flap blocks the air which causes air's dynamic pressure to manifest as static pressure. A perfect seal is not possible against the gravel between the rails. Figure 4 similarly summarizes the impact of Flap % on L/D efficiency.

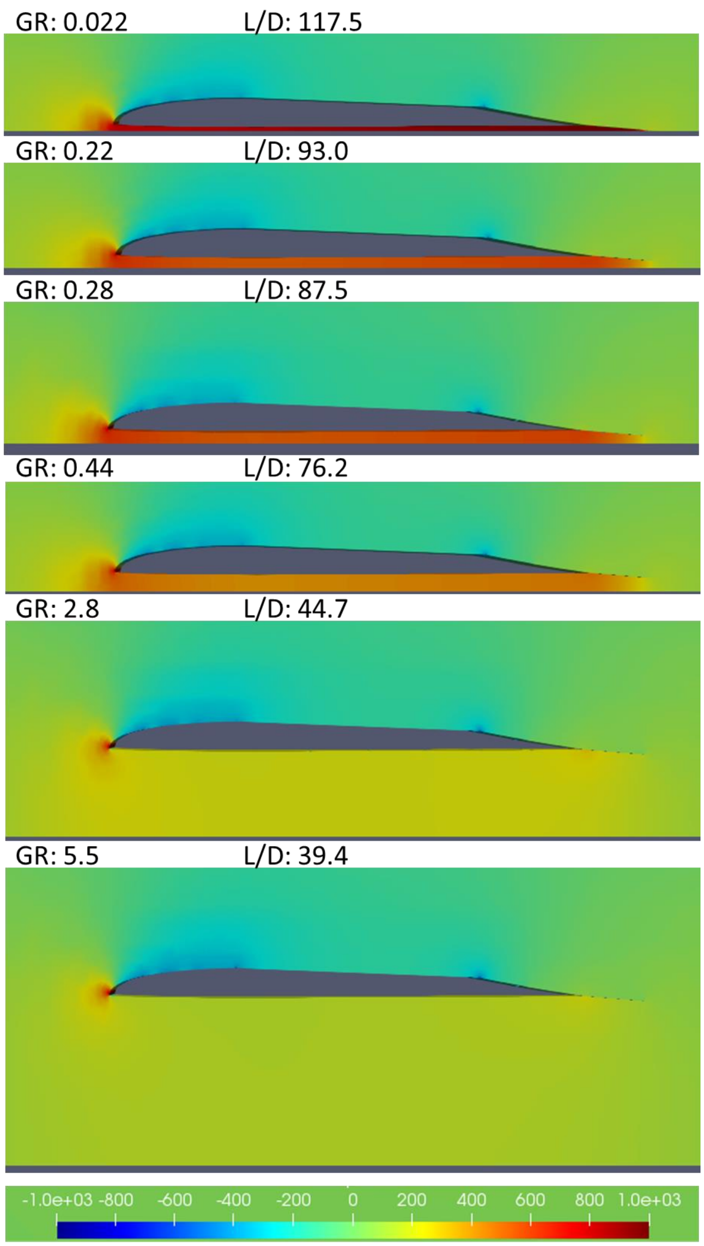

Figure 3. Pressure profiles of railcar airfoil flying at six different clearance ratios above the ground.

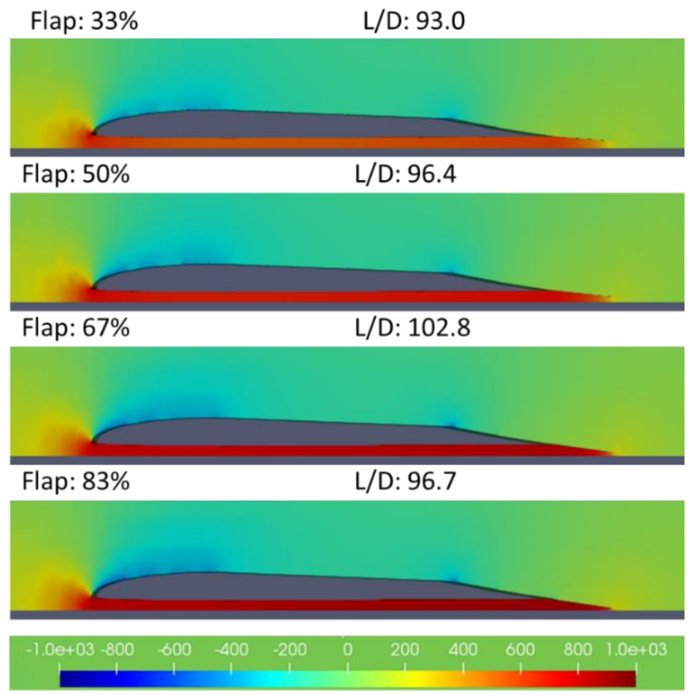

Figure 4. Pressure profiles of railcar airfoil flying three different at four different flap angles and flap % above the ground.

Table 1. Comparison of L/D and C_l of thick airfoil simulations including performance of Figure 3 and Figure 4 airfoils and conditions. Simulated length is 6.4m (including flap). P_{avg}: average pressure in Pa at 3.2m along the airfoil.

Clearance ratio	Flap %	C_l	C_d	P_{avg} (Pa)	L/D
0.022	83.3%	1.322	0.0113	1172	117.5
0.055	66.7%	1.187	0.0104	1031	113.7
0.11	50.0%	1.052	0.0098	886	106.8
0.165	40.0%	0.963	0.0097	777	99.4
0.22	33.3%	0.893	0.0096	707	93.0
0.275	28.6%	0.845	0.0097	666	87.5
0.44	20.0%	0.739	0.0097	543	76.2
1.1	9.1%	0.568	0.0100	369	57.0
2.75	3.8%	0.466	0.0104	271	44.7
5.5	2.0%	0.420	0.0107	196	39.4
∞	0.0%	0.296	0.0139	N/A	21.2
Flap Percentages at gap ratio of 0.22 Clearance Ratio					
0.165	50.0%	1.050	0.0109	893	96.4
0.11	66.7%	1.234	0.0120	1041	102.8
0.055	83.3%	1.304	0.0135	1105	96.7

Figure 5 summarizes the trends in performance of the 2D airfoil studies. Lower gap and clearance ratios lead to higher pressures and high Cl. Increased Flap % leads to higher C_l by more thoroughly converting air's dynamic pressure into higher pressures within the compartment. Increases in C_d are the result of the higher pressure in the compartment acting over the vehicle's increased frontal projection of area (including the frontal projection of the flap and carriage base slope).

The peak in L/D versus Flap % is expressed by a fit of C_l divided by C_d and exacerbates the slight curvature in the coefficients' fits of model lines for C_l and C_d. More specifically, the decrease in L/D at high Flap % is the phenomena of interest; it is due to the narrowing gap between the lower edge of the flap and the ground. The likely interpretation is that shear drag, which is typically less than 1% the magnitude of form drag, increases as the boundary layer for shear flow is encroached.

Likewise, the encroachment on the boundary layer explains the sharp increase in drag at low gap ratios. It is possible turbulent flow phenomena contribute to added drag as the gap decreases.

The increase in C_d with increasing clearance ratio is a more complex phenomenon. It is likely due to higher pressures forming on lower frontal surfaces of the vehicle. These higher pressures expand upward, and when the expansion is next to a surface having pitch of greater negative slope at lower portions of the vehicle's front; this leads to more diverging of air flow on the upper frontal surfaces. More diverging air flow from frontal surfaces leads to induced thrust which decreases drag.

Minimal effort was made to optimize the front surface shape of the vehicle, and it is possible that the increase in C_d with increasing clearance ratio is an artifact of a non-optimal design. But optimal design depends on the use of the vehicle where a vehicle designed for service only over rails is different from a vehicle designed for substantial service in free flight.

While standard deviations in the CFD results are low, deviation from the continuous trends of fit lines manifests at expanded y-axis scales and with high L/D. The highest L/D are a result of low C_d, and low C_d are a result of induced thrust reducing the total drag. Total drag is the drag as calculated from surfaces minus induced thrust calculated from surfaces, and subtracting two small numbers leads to increased standard deviation, even within CFD simulations.

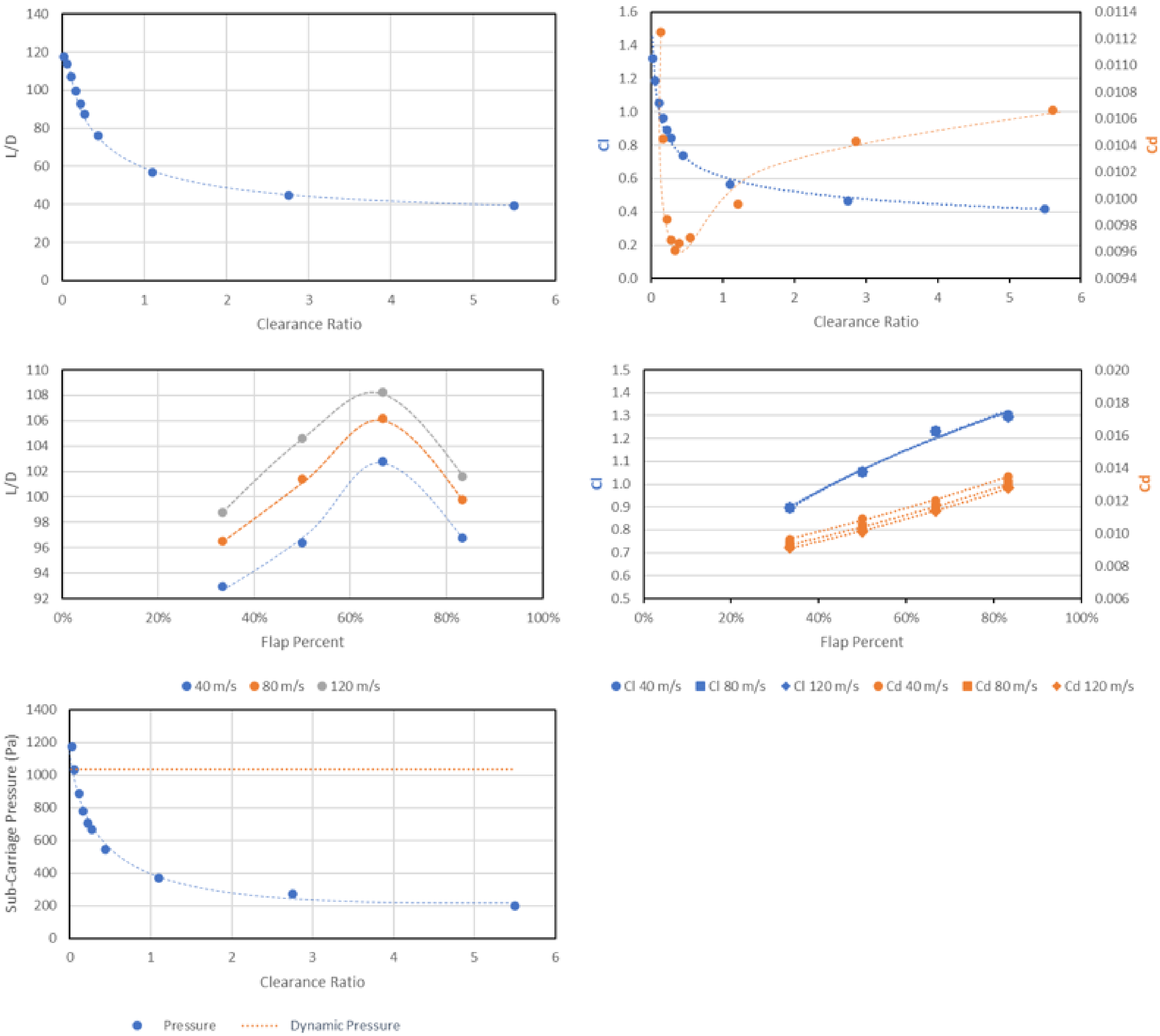

Figure 5. Correlation graphs dependent on clearance ratio and flap percent. A and B relate trends in L/D vs clearance ratio and flap percent respectively. B and D relate C_l and C_d to clearance ratio and flap percent respectively. The impact of flap percent is presented at 40, 80, and 120m/s. E displays the average pressure at 3.2m along the airfoil with a reference line of the dynamic pressure.

3D CFD Studies – The 2D CFD studies generated exceptionally high L/D efficiencies. By example, airliners have excellent L/D efficiencies, with an industrial average near 15 for optimal cruising. Values of 2D airfoil L/D exceeding 100 are >7x that of airliners. A priority emerges on preserving the high L/D efficiency from losses over side edges in transition to 3D applications.

Figure 6 summarizes the pressure profiles and L/D for a lifting body vehicle having a 4' 8" fenced lower middle section, a cabin-airfoil-cross-section to a span of 10.5', and upper surface wing extensions about 2' on from both sides of the cabin. In free flight the L/D is 5.2, at 0.022 CR over rails the L/D is 41.8, and with an upper surface fan propulsor at the 0.022 CR the L/D can be increased to >60.

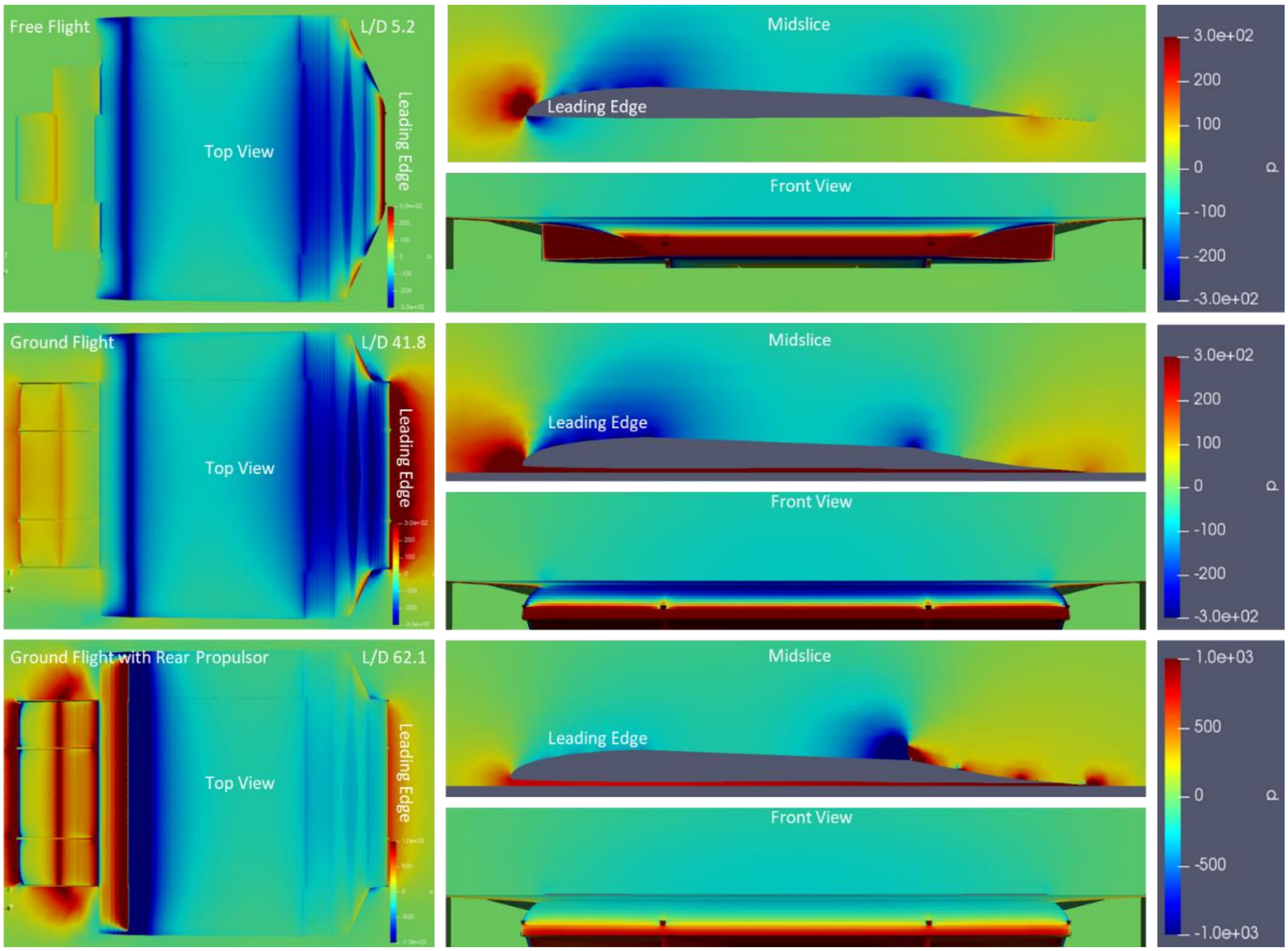

Figure 6. 3D CFD of WIG railcar over ground versus in free flight illustrating impact of ground effects on pressure profile (CR - 0.022).

For an 8' cabin height, the 0.022 clearance ratio translates to a vertical gap of about 2" between the flap and ground. Fences will be vertically aligned above the rail. Since the fence can be designed to have a lower fence section that slides vertically within an upper fence section, it is possible to have the lower fence section use wheels to block blunt contact of the fence with the rail; the result is the ability to operate with gaps less than about 0.5" to reduce edge loss effects. The 2" gap is a conservative design where lower gaps can increase L/D depending on rail specifications.

The 2D airfoil prototype was modified during the course of 3D studies to continuously decrease the gap in the direction of airflow; this is observable by comparing the side views of the compartment gaps. A continuously decreasing gap at a pitch of about 0.25° was a measure taken to compensate for side edge losses.

Lower Surface Constriction of Flow – A flap is used to constrict flow and create pressure in the compartment. In principle, the pitch of the lower surface could decrease to attain an area of close approach to the ground in the compartment's trailing section to attain pressure profiles similar to those generated with a flap. Advantages of the flap include reduced close-proximity shear drag, use as an adjustable control surface, and designs to allow unintentional contact with the ground with minimal disruption to flight.

Optimal configurations use both a flap section and a low surface pitch (e.g., 0.2° or lower). The optimal lower surface shape depends on the extent of lift pressures lost through fence-rail gaps.

Extended Discussions and Implications

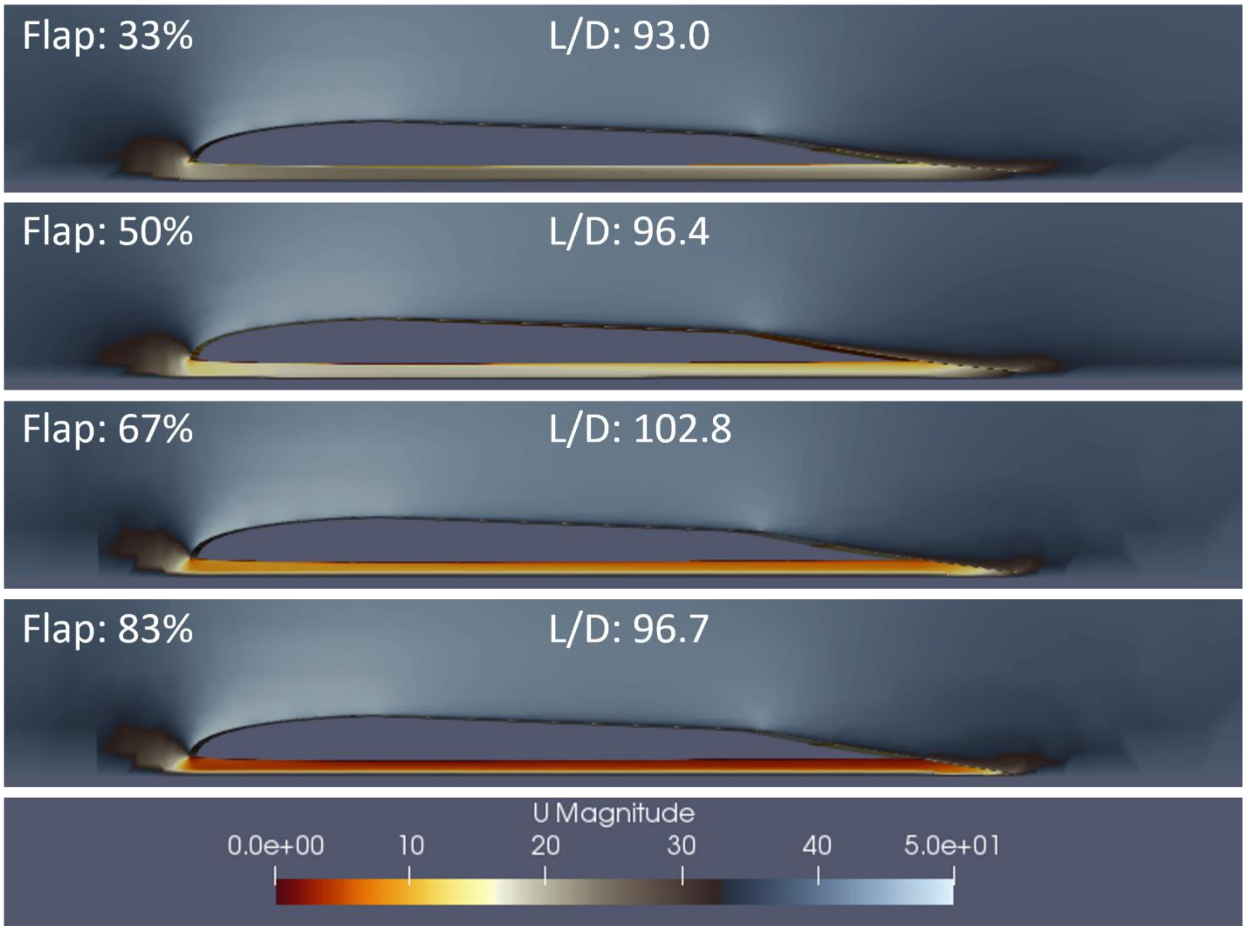

Figure 7. Velocity on Flap coverage velocity profiles with airfoil as reference frame (0 is airfoil going 40m/s) at different flap coverage percentages. Original clearance ratio is 0.22 and decreases by 25% in descending airfoils.

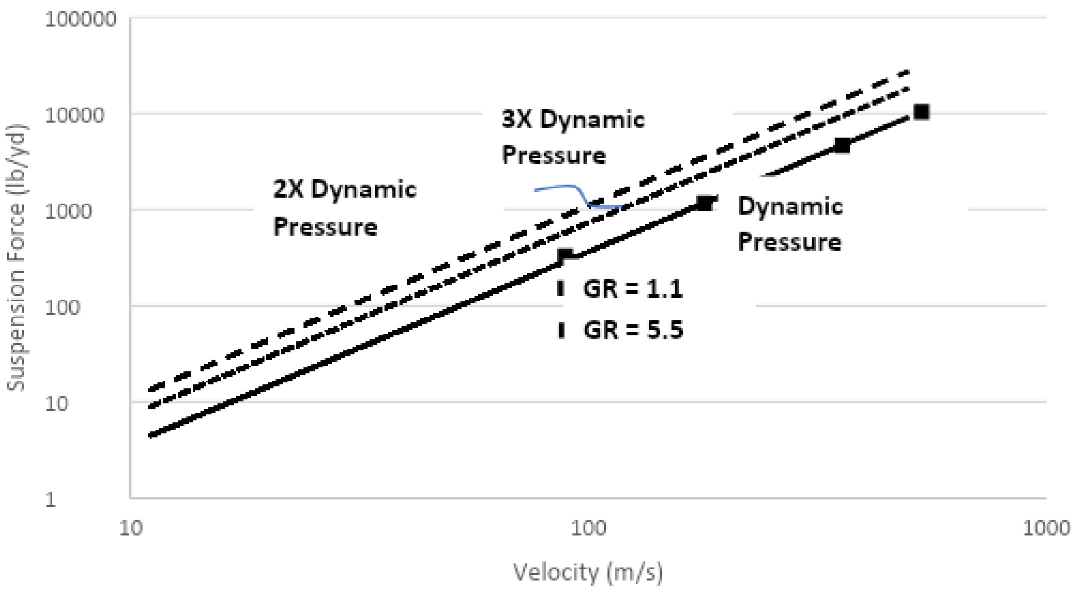

Figure 8. Calculation of lift force per yard of vehicle length using only 4' 8" wide lift force from the rails. Data are at CR = 0.022 unless otherwise indicated.

Table 2. Comparison of L/D, C_l, and P of airfoils at increasing velocity. The 6.4m cabins were at the 0.022 CR with velocities between 40 and 240m/s.

Clearance ratio	Flap %	Velocity (m/s)	Cl	Cd	L/D	P_{avg} (Pa)	Q (Dynamic P)	P_{avg}/ Q
0.022	83.3%	40	8.46	0.0720	117.5	1175	1034	1.136
0.022	83.3%	80	33.5	0.275	121.6	4637	4138	1.121
0.022	83.3%	160	133	1.06	125.6	18344	16550	1.108
0.022	83.3%	240	297	2.32	127.8	41017	37238	1.101

Maximum Lift Coefficients –The dynamic pressure for the free steam air flow (40 m/s) of Table 2 is 1030 Pa which is comparable to the 1172 Pa compartment pressure for the narrowest gap of Table 2. This identifies that as the gap height approaches zero, the air velocity in the gap also approaches zero relative to the airfoil (see Figure 7) and all the dynamic pressure is transformed to lift-generating pressure. Data at 80, 160 and 240 m/s follow the dynamic pressure line (table 2). This performance validates the CFD simulations and transforms sophisticated Navier Stokes calculations to a phenomenon that can be associated with more basic physics.

Minor positive deviations from the dynamic pressure line are possible when air flow is deflected downward for additional upward force generation.

Equations 1 and 2 show the similarity of the equations defining dynamic pressure and the lift coefficient. The vehicle's lower surface contributes a magnitude of 1.0 to the lift coefficient (C_l) as the gap and clearance ratios approach zero.

$$P_D = \frac{1}{2}\rho u^2 \quad 1$$

$$\frac{L}{A} = \frac{1}{2}C_l \rho u^2 \quad 2$$

Figure 8 summarizes lift in terms of lbs. of upward force per yard of vehicle length for C_l = 1.0, 2.0, and 3.0. The assumption is that a well designed vehicle can approach C_l=2 for the portion of the vehicle above the 4' 8" track span ("track planform") due to lift on both upper and lower surfaces. The surfaces outside the track planform would be less efficient in generating lift with the identified upper dashed line being a reasonable target performance.

Table 3. L/D and P of scaling airfoils at 40m/s

Model Length	P_{avg}	L/D
0.8m	1306	92.26028
6.4m	1218	112.0143
12.8m	1191	109.2904
25.6m	1171	105.8494

Allowing 400 lb for each passenger (including vehicle weight) for each yard of length results in 1600 lb/yd for a carriage four seats wide which is attained at 121 mph along the upper curve. At 50 mph, the upper curve is 274 lb/yd, and a two-passenger vehicle (800 lb) would need to be about 3 yd long at 50 mph to have full aerodynamic suspension. These values provide base case target values to initiate optimization. The potential L/D scales well as the length of the vehicle extends, allowing for numerous applications to be developed based on target weight and passenger counts.

The highest efficiencies are achieved only with aerodynamic suspension plus any free suspension supplemented by a linear motor for propulsion. CFD simulations of flight reveal that L/D is independent of velocity for reasonably wide ranges of velocity, and so, energy efficiency is substantially independent of velocity once flight velocities are achieved when the entire vehicle is designed to convert form drag into aerodynamic lift. Under these conditions, power requirements are linear with speed.

Preliminary studies of digital prototypes in tunnels reveal that tunnel walls can block upward and spanwise losses of lift which further increases L/D. C_l has a natural maximum of 2.0 due to a contribution of 1.0 for upper surfaces and 1.0 from lower surfaces. That 2.0 limit can be approached for all lift surfaces (including those outside the planform) and C_d decreases due to induced thrust possible under conditions with benefits from tunnel walls. Preliminary studies identify that L/D in excess of 100 are possible for aircraft in optimally designed tunnels.

Preferably, most of the propulsion is from distributed propulsion in the form of propellers or fans because the pressures generated by these propulsors can be leveraged to increase L/D [12, 13]. At speeds lower than the critical velocities for full aerodynamic suspension, suspension is preferably supplemented by rubber tires or propulsor thrust vectoring; the former for vehicles that would not leave the tracks and the latter for vehicles designed for vertical or short runway landing and takeoff and landing.

Translating High L/D to Reduced Energy and Costs – Energy expended in transportation is consumed to overcome drag forces which are characterized as either drag or friction, including: a) wheel-related friction, b) shear drag, c) form drag, d) electromagnetic drag/losses, and e) fan/propeller losses. A base case WIG railcar is assumed to have >95% of the weight supported by aerodynamic lift during transit over rails; the remaining <5% is reserved for use to enhance control-of pitch, yaw, and roll to stay on the tracks. The following apply in comparing aerodynamic lift suspension to alternatives:

1. Shear drag is typically less than 1% of the form drag needed to provide aerodynamic lift.
2. Wheel-related friction is of low impact when wheels support less than 5% of a light-weight vehicle.
3. Electromagnetic drag is of low impact when magnetic forces support less than 5% of a light-weight vehicle.

In this base case analysis, form drag emerges as the primary force to overcome during transit. The following provide a basis for the form drag of a WIG railcar being less than the form drag of a train:

1. Form drag is primarily related to the projected frontal area, and since a WIG railcar has about half the height of a train due to the absence of a heavy-duty chassis needed to absorb and transfer the train's collective mass.
2. A WIG railcar streamlines air flow on upper, lower, and side surfaces while a train typically does not streamline air flow on lower surfaces; consequently, a WIG railcar should have lower drag than a wheel-based train of a similar projected frontal area.

The conclusion is that a Flying Train will have lower per-passenger-mile energy consumption than either wheeled or maglev trains. Versus airliners, higher L/D and lower vehicle weights per passenger capacity (i.e., less fuel and battery weight due to transfer of electrical power during transit) result in lower per-passenger-mile energy consumption than airliners. Preliminary estimates are that passenger-mile energy consumption of a WIG railcar would be half that of contemporary trains and one seventh that of airliners—these numbers are based on a comparison of the CFD results of this paper to transport energy efficiencies published by the U.S. Department of Energy.[14, 15]

Ground Effect Flight - Realizing efficient aerodynamic lift includes both generating aerodynamic lift and preventing losses of that lift. For airplanes in free flight at higher altitudes, loss of lift due to upward and downward flow of air is an unavoidable loss. In close proximity to the ground, the ground successfully blocks the downward flow of air. In addition, the rails of a railway will block most of the loss of lift due to flow of air over side edges. And so, it is possible for a WIG railcar to achieve higher L/D efficiency than the best airliner.

The 2D CFD results of this paper apply to flight over open ground, highways, and water. Several companies are developing ground effect aircraft for use over water. [16-20]Calm water provides a flat surface which is important to realize the upper-end potential of ground effect aircraft. However, waves limit the extent to which the aircraft are able to approach the water.[21-27] For example, an 8' gap could fly over 6' waves; however, the 8' gap for a 2' thick airfoil realizes less than 25% of the dynamic pressure limit that ground-effect flight over rails should be able to achieve. The comparison of the WIG railcar to ground effect over water exemplifies rail's advantages of flight with low gap ratios and blocking of side-edge losses.

Also, today's designs for ground effect aircraft over water use tube-and-wing designs; those designs are a manifestation of flawed theories of lift that focus on bending of air around NACA-type airfoils. [28] The design of the WIG railcars of instant paper are based on Heuristics 1-4. The design heuristics identify the value of a near-horizontal surface for achieving high L/D efficiency. The fence on the near-horizontal lower surface of preferred ground-effect aircraft blocks losses and has utility for most ground effect aircraft.

For free-flight aircraft, winglets are commonly used while fences are not. Fences are useful when high lift forces are present along a considerable length of the vehicle, as is the case with ground-effect aircraft having extensive nearly-flat surfaces under fuselages. A natural extension of ground-effect aircraft are sea planes that fly with these improved ground effect designs which manifest as hydrofoil-like ships that take flight.

Efficiency versus train units – Factors that decrease efficiency of today's passenger trains relative to a WIG railcar include: a) height and weight associated with undercarriages, b) wheel friction, c) absence of streamlining on lower surfaces, and d) non-optimal form drag. For a short train, these factors cause the train to have a lower per-passenger efficiency than a WIG railcar. In principle, a long train could have higher per-passenger efficiency than a WIG railcar; however, even a longer train would tend to have lower efficiency due to intermittent stops consistent with the large number of passengers.

Table 4 compares the projected efficiency and speeds of the WIG railcar to other modes of transit.

The results of this paper identify that L/D values in excess of 60 are possible; considerably better than is possible with today's airliners and trains. Higher speeds are possible since air suspension with minor rubber tire supplement will cushion bumps in the rails; those higher speeds are possible on subway, light rail, and heavy rail tracks. Versus the competition, WIG rail stands out in aspects of: higher efficiency, higher speeds, and improved access while avoiding airport congestion.

Table 4. Comparison of fuel economies. Values are estimates from a range of sources.

Mode	Btu/Passenger Mile	Speeds (mph)	L/D

Quadcopter		0-70	5
Helicopter		0-120	7
Typical Air Taxi	>5000	60*-120	5-12
Light Aircraft		80-300	11
2025 Ground Effect over Water		60-90	14
HS-Drone Ground-Effect of Water	600	80-300	>30
Passenger Car[20]	1500-2000	0-80	
WIG Railcar	400	0-250	40 to >60
Intercity and Commuter Rail [20]	800-1600	0-120	
Airliner [20]	2400	140*-520	15

Contrary to common descriptions on aircraft efficiency, the L/D efficiency of a lifting body does not decrease significantly with decreased pressures or higher altitudes. The L/D efficiency of a well-designed lifting body at 1 atm of pressure at ground level is about the same as at the 0.2 atm of typical jet cruising altitudes. Lift and drag generation are proportional to both density and velocity squared; hence L/D is substantially independent of air's density which is proportional to pressure.

$$D = \frac{1}{2} A C_D \rho u^2 \qquad 3$$

$$L = \frac{1}{2} A C_l \rho u^2 \qquad 4$$

An accurate consideration of "increased efficiency with higher altitudes" is that tube-and-wing designs are more efficient at higher altitudes since the drag on the tube has little aerodynamic lift and drag decreases with lower pressures.

The cruising L/D efficiency of a WIG railcar depends on many factors, of which, a design that transforms the higher pressures forward on the railcar to lower pressures on forward sections of the railcar are most important. These lower pressures generate induced thrust which subtracts from drag in the manifesting of L/D efficiency.

Hybrid Wheel-Aerodynamic Suspension – Cruising with 1% to 5% wheel suspension allows the contact of the wheel to control the rail-fence gaps, where lower wheel-fence gaps provide the greatest efficiency. A 0.02 clearance ratio translates to a 2.5 cm gap with a 2.5 m lifting body fuselage height. As velocity decreases, wheels would provide increased percentages of suspension versus the suspension provided by air's dynamic pressure.

Having at least part of the railcar lift supported by wheels simplifies pitch, roll, and yaw control. In the absence of wheels to provide these controls, vertical movement of fence sections relative to the lower surface of the fuselage and the changing of the angle of the trailing flap emerge as methods with respective control surfaces.

Bumps in tracks are inherently dampened with aerodynamic suspension supporting >90% of the weight, enabling use of lower-grade tracks and higher velocities. Most operating conditions of flying railcars as highlighted retain a gap greater than most rail tolerances.[29-31] The tracks allow access within cities using existing subway and rail infrastructure versus air transit which does not have access throughout cities. The combination of high flight efficiency, direct use of grid power, and safety when engaging tracks makes rail guided transit preferred over free flight when tracks are available. A further advantage of flight that directly uses grid power is that the weight of the fuel does not detract from energy-per-passenger-mile efficiency.

Preferred “WIG railcars” would be light weight—absent the heavy-duty undercarriages of train carriages; these vehicles are in the R&D stage. Tracks maintained for train service would be suitable for use with high-speed WIG railcars. WIG-railcars with supplemental wheel suspension can be drop-in service replacements or expansions. The evolutionary path of WIG railcars includes seamless switching from different track systems and to highways due to the ability of aerodynamic lift to provide full suspension.

Conclusions

All aircraft are limited in flight efficiency by the loss of aerodynamic lift pressures in vertical and lateral directions which results in typical upper-end L/D efficiencies of about 18. During flight close to the ground, the ground blocks losses in the downward direction; and with flight that engages railway tracks, the tracks block lateral losses. The rails provide a unique opportunity to block losses of lift pressures while engaging the tracks with close clearances (e.g., 2 cm for fence-rail clearances) to attain L/D efficiencies in excess of 60. This is about twice as efficient as contemporary high-speed rail. Good lifting-body designs for WIG railcars do not suffer from reduced efficiency due to operation at ground level pressure versus higher cruising altitude pressures of jets.

Key features of the WIG railcar toward achieving high L/D efficiency are: a) a lower compartment defined by side fences and a trailing edge flap, b) a forward section that both directs air’s dynamic pressure into the lower compartment and generates induced drag on the upper frontal surfaces, c) fence height controlled in tight tolerances (e.g. 2 cm) with the railway track, and d) upper surface distributed propulsion that both generates lift on upper surfaces and further increased induced thrust.

References

[1] Leifsson, L., Ko, A., Mason, W., "Multidisciplinary Design Optimization for a Blended Wing Body Transport Aircraft with Distributed Propulsion," 2011,

[2] Krishna, Y.C., and Venkatesh, T.N., "Numerical investigation of aerodynamically efficient wing tip-mounted propeller configuration using coupled RANS–BEM approach," *Aircraft Engineering and Aerospace Technology,* Vol. 95, 2023,

[3] Winslow, J., Otsuka, H., Govindarajan, B., "Basic Understanding of Airfoil Characteristics at Low Reynolds Numbers (104–105)," *Journal of Aircraft,* Vol. 55, 2017, pp. 1-12.

[4] Klose, B., Spedding, G., and Jacobs, G., "Direct numerical simulation of cambered airfoil aerodynamics at Re = 20,000," 2021,

[5] Michna, J., and Rogowski, K., "Numerical Study of the Effect of the Reynolds Number and the Turbulence Intensity on the Performance of the NACA 0018 Airfoil at the Low Reynolds Number Regime," *Processes,* Vol. 10, 2022, pp. 1004.

[6] Lee, D., Nonomura, T., Oyama, A., "Comparison of Numerical Methods Evaluating Airfoil Aerodynamic Characteristics at Low Reynolds Number," *Journal of Aircraft,* Vol. 52, 2015, pp. 296-306.

[7] Suppes, A., Suppes, G., Lubguban, A., "Kinetic Theory of Gases: Explanation of Aerodynamic Lift," *Under Review at Journal of Chemical Education,* 2024,

[8] Loyalka, S.K., and Chang, T.C., "Sound-wave propagation in a rarefied gas," *Physics of Fluids,* Vol. 22, 1979, pp. 830.

[9] Loyalka, S.K., "Motion of a sphere in a gas: Numerical solution of the linearized Boltzmann equation," *Physics of Fluids: Fluid Dynamics,* Vol. 4, No. 5, 1992, pp. 1049-1056.

[10] Garcia, R., and Siewert, C., "The linearized Boltzmann equation: Sound-wave propagation in a rarefied gas," *Zeitschrift Fur Angewandte Mathematik Und Physik,* Vol. 57, 2005, pp. 94-122.

[11] Loyalka, S., "On Boundary Conditions Method in the Kinetic Theory of Gases," *Zeitschrift Naturforschung Teil A,* Vol. 26, 2014, pp. 1708.

[12] Suppes, G., and Adam, A., "Understanding Thin Cambered Airfoils and their Solar Aircraft Applications," *J. Aircraft,* Submitted for Review (preprint available),

[13] Suppes, A., and Suppes, G., "Thermodynamic Analysis of Distributed Propulsion," *Cnet,* Submitted for Review (preprint available),

[14] Anonymous "Energy efficiency in transport," [online database]https://en.wikipedia.org/w/index.php?title=Energy_efficiency_in_transport&oldid=1144848549#cite_note-ORNL/TM-2020/1770-135 [cited Mar 19, 2023].

[15] Anonymous "Fuel economy in aircraft," [online database]https://en.wikipedia.org/w/index.php?title=Fuel_economy_in_aircraft&oldid=1180671286 [cited Nov 6, 2023].

[16] Suppes, G., and Suppes, A., "Fixing Airplane Science - If we would have only known," Kindle by Amazon, Charlottesville, VA, 2024,

[17] Suppes, A., and Suppes, G., "Highly-Efficient Low-AR aerial vehicles in urban transit," *Proceedings of the 2014 Transportation Research Board Annual Meeting,* January, 2024,

[18] Correspondents, B.N.N., "Liberty Lifter: DARPA's Ground Effect Aircraft Revolution," [online database]https://bnnbreaking.com/tech/liberty-lifter-darpas-ground-effect-aircraft-revolution [cited Feb 12, 2024].

[19] D'Urso, S., "DARPA Developing Wing-In-Ground Effect Cargo Seaplane," *The Aviationist,* 2023,

[20] Wiriadidjaja, S., Zhahir, A., Mohamad, Z., "Wing-in-ground-effect craft: A case study in aerodynamics," *International Journal of Engineering and Technology(UAE),* Vol. 7, 2018, pp. 5-9.

[21] Hu, H., Zhang, G., Li, D., "Shape optimization of airfoil in ground effect based on free-form deformation utilizing sensitivity analysis and surrogate model of artificial neural network - ScienceDirect," *Ocean*

Engineering, Vol. 257, 2022, pp. 111514.

[22] Deviparameswari, K., Meenakshi, S., Akshay Kumar, N., "The Effects of Ground Clearance and Boundary Layer Blockage Factor on the Aerodynamics Performance of the Hyperloop Pod and Transonic Ground-Effect Aircraft | AIAA AVIATION Forum," *AIAA Aviation Forum,* 2021,

[23] Blain, L., "Regent to debut its hydrofoiling ground-effect Seagliders in Hawai'i," [online database]https://newatlas.com/aircraft/hawaii-seaglider/ [cited Mar 8, 2024].

[24] Su, S., Shan, X., Yu, P., "The compressibility effects on the inherent stability of Wing-In-Ground crafts," *AIAA SciTech Forum,* 2021,

[25] Qu, Q., Wang, W., Liu, P., "Airfoil Aerodynamics in Ground Effect for Wide Range of Angles of Attack," *AIAA Journal,* Vol. 53, No. 4, 2015,

[26] Wang, J., Chen, R., Yu, Z., "Ground test and numerical investigation on aerodynamic performance of a quad tilt-rotor aircraft in ground and water effects - ScienceDirect," *Ocean Engineering,* Vol. 289, No. 2, 2023, pp. 116169.

[27] Zou, Y., You, C., Tan, X., "Design and implementation of a gliding cross-domain vehicle," *Ocean Engineering,* Vol. 280, 2023, pp. 114549.

[28] Anonymous "NACA airfoil," 2023,

[29] Noland, J.K., "Prospects and Challenges of the Hyperloop Transportation System: A Systematic Technology Review," *IEEE Access,* Vol. 9, No. 2021, pp. 28439-28458.

[30] Zyga, L., "Ground-effect 'plane-train' flies inches above the ground (w/ video)," [online database]https://phys.org/news/2011-05-ground-effect-plane-train-flies-inches-ground.html [cited Mar 8, 2024].

[31] Yaghoubi, H., Barazi, N., Kahkeshan, K., "Technical Comparison of Maglev and Rail Rapid Transit Systems," *The 21st International Conference on Magnetically Levitated Systems and Linear Drives,* 2011, pp. 5.

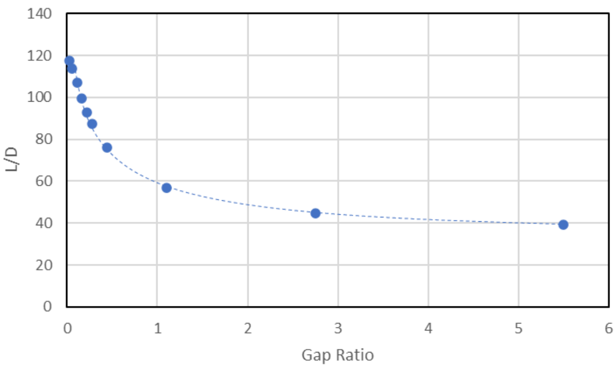
L/D
Gap Ratio

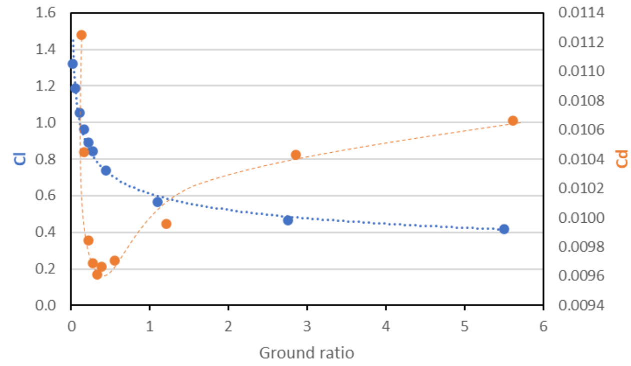
Cl
Cd
Ground ratio

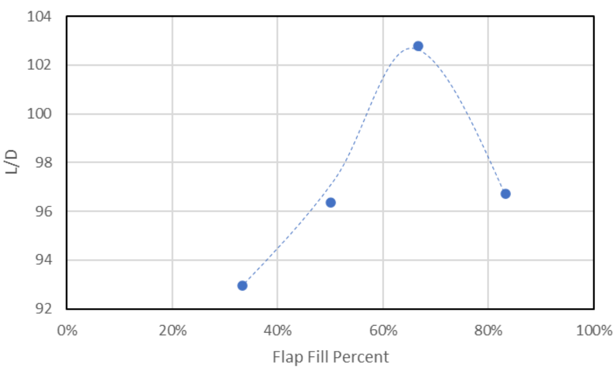
L/D
Flap Fill Percent

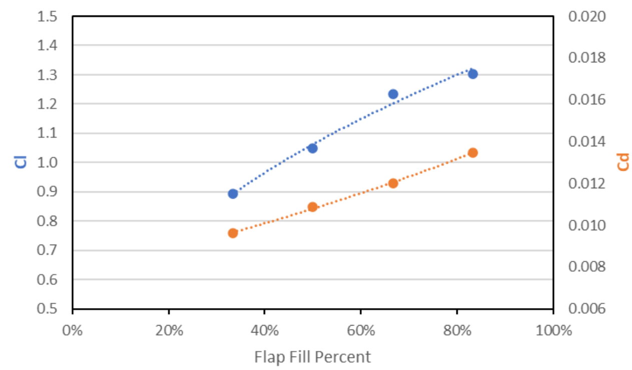
Cl
Cd
Flap Fill Percent

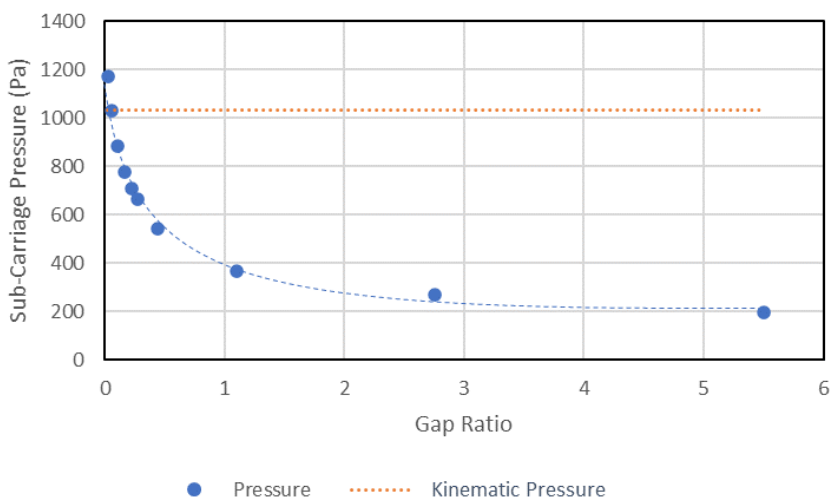
Sub-Carriage Pressure (Pa)
Gap Ratio
Pressure
Kinematic Pressure